Climate warming and interannual variability of phytoplankton phenology in the Northern Red Sea

Thesis by

John Anthony Gittings

In Partial Fulfillment of the Requirements

For the Degree of

Master of Science

King Abdullah University of Science and Technology, Thuwal,
Kingdom of Saudi Arabia

EXAMINATION COMMITTEE PAGE

The thesis of John Anthony Gittings is approved by the examination committee.

Committee Chairperson: Professor Ibrahim Hoteit
Committee Members: Dr Dionysios Raitsos, Professor Michael Berumen, Professor Burton Jones

ABSTRACT

In agreement with global patterns of climate change and increasing temperatures in the tropical oceans, the Northern Red Sea (NRS) has been warming over the last few decades. Using 18 years of remotely-sensed chlorophyll-a data (Chl-a, an index of phytoplankton biomass), we investigate the potential impacts of climate warming on phytoplankton abundance and phenology in the Northern Red Sea by exploring the mechanistic links with the regional physical environment. The results of the analysis reveal that, in accordance with other tropical ecosystems, phytoplankton biomass in the NRS will decrease in response to warmer climate scenarios. This is attributed to lower heat fluxes (heat loss to the atmosphere) during the bloom period, and enhanced vertical stratification, which prevents vertical mixing of nutrients into the euphotic layer. In addition, we show that during warmer conditions (when heat fluxes are weakened), the winter bloom initiates significantly later (by up to 10 weeks) and its duration is considerably reduced. The biological implications of alterations to phytoplankton phenology may include increased larval mortality of pelagic species, reduced recruitment, fisheries impacts and changes to community structure.

TABLE OF CONTENTS

LIST OF FIGURES

1. INTRODUCTION

Sea surface temperature (SST) in the tropical and subtropical oceans has increased abruptly over the last 30 years, and is predicted to keep rising (1-2°C per century, Hoegh-Guldberg, 1999) primarily due to the anthropogenic enhancement of greenhouse gas concentrations in the atmosphere [Solomon *et al*., 2007]. The Red Sea Large Marine Ecosystem is going through a step-wise warming phase that began in the mid-1990's and has been associated with increasing regional air and Northern Hemisphere temperatures [Raitsos *et al*., 2011]. Despite it's naturally high temperatures (up to 35.0°C during summer, Berumen *et al*., 2013), the Red Sea is not invulnerable to warming events. Furby *et al*. [2013] reported widespread coral bleaching (the loss of symbiotic algae from coral tissue) in the central east Red Sea during the summer of 2010 - a period of prolonged anomalously high temperatures. A reduction in skeletal growth (calcification) rates of Red Sea corals has also been linked with rising sea surface temperatures [Cantin *et al*., 2010]. Alterations in the community structure of coral reef communities may also be expected in association with increasing global temperatures [Done, 1999].

Phytoplankton, the microscopic algae situated at the base of the marine food web [Armbrust *et al.*, 2004], are a vital component of the Red Sea marine ecosystem. Unlike the temperate oceans (light-limited regions), phytoplankton in tropical marine ecosystems are primarily nutrient limited. Consequently, phytoplankton abundance and primary productivity in the tropics are expected to decrease under scenarios of global warming as a result of increased stratification, diminished vertical mixing and reduced nutrient supply to the euphotic zone [Behrenfeld *et al*., 2006, Doney, 2006].

Chlorophyll-a (Chl-a), the universal pigment found in the light-harvesting chloroplasts of algae [Hurd *et al*., 2014] is a good indicator for the presence of phytoplankton biomass, and has been used widely in the past to estimate phytoplankton abundance in aquatic ecosystems [Suzuki and Ishimaru, 1990]. The collection of adequate *in situ* Chl-a measurements for assessing large-scale phytoplankton dynamics may be time-consuming and expensive. An alternate method is the use of satellite ocean colour remote sensing, from which Chl-a concentrations can be quantified synoptically [Sathyendranath and Platt, 1997].

Previous research using remotely-sensed ocean colour has revealed that the distribution of Chl-a across the Red Sea is spatially heterogeneous, enabling the division of the Red Sea into biological provinces [Raitsos *et al.,* 2013]. The Northern Red Sea province (NRS) exhibits a distinct seasonality of surface Chl-a, with highest chlorophyll-a concentrations occurring during winter [Acker *et al*. 2008; Raitsos *et al*., 2013]. Colder atmospheric conditions contribute to significant heat loss over the region, which generates convective mixing (overturning) and the transport of nutrients from deeper waters into the euphotic zone [Sofianos and Johns, 2003; Triantafyllou *et al*., 2014].

Aside from an understanding of seasonality, the NRS is biologically unexplored in the context of large-scale phytoplankton dynamics, particularly at an interannual scale. One approach used to monitor the phytoplanktonic component of the marine ecosystem is the study of phytoplankton phenology [Racault *et al*., 2012]. Assessing phytoplankton phenology – the timing of phytoplankton blooms – can serve as a useful indicator for assessing the condition of the pelagic ecosystem interannually [Platt *el al*., 2003; Platt and Sathyendranath, 2008]. The fitness and recruitment of organisms at higher trophic

levels is ultimately dependent on temporal synchrony with food availability (match – mismatch hypothesis, Cushin*g*, 1974; Winder and Schindler, 2004]). Thus, interannual fluctuations in the timing of bloom initiation, termination and duration can have far-reaching ecosystem impacts. Indeed, a delayed initiation of the spring bloom at the Eastern Nova Scotian shelf has been linked to a decrease in the survival rate of larval fish [Platt *et al*., 2003]. The decomposition of phenological relationships may ultimately lead to an alteration in marine food web structure and changes that are apparent at an ecosystem level [Edwards and Richardson, 2004].

Warmer climate phases (El Niño conditions) have been linked with increased productivity over a large part of the Red Sea as a result of increased (wind-induced) horizontal advection of nutrients [Raitsos *et al*., 2015]. However, the NRS is the only region that does not imitate this pattern and the biological response of warmer conditions in the region is not yet understood. In this respect, the NRS is the only part of the Red Sea where phytoplankton dynamics follow a typical tropical regime, where warmer, stratified conditions decrease phytoplankton abundance [Doney, 2006; Raitsos *et al*., 2015].

In this study, the long-term (> 17 years) interannual variability of phytoplankton phenological metrics (the timings of bloom initiation, termination and duration), as well as absolute Chl-a concentrations, are investigated for the first time in the NRS. Furthermore, a combination of modeled and satellite data is used to explore the mechanistic links between phytoplankton phenology and the regional physical environment. The implications of warmer conditions on phytoplankton in the NRS are also considered.

2. METHODOLOGY

2.1. Study area

Geographical limits of the NRS were chosen based on the Red Sea provinces defined by Raitsos *et al.* [2013]. For the purpose of this study, the Gulfs of Aqaba and Suez were not included in analysis. The NRS is defined as the region between 25.5°N - 27.8°N and 33°E - 37°E.

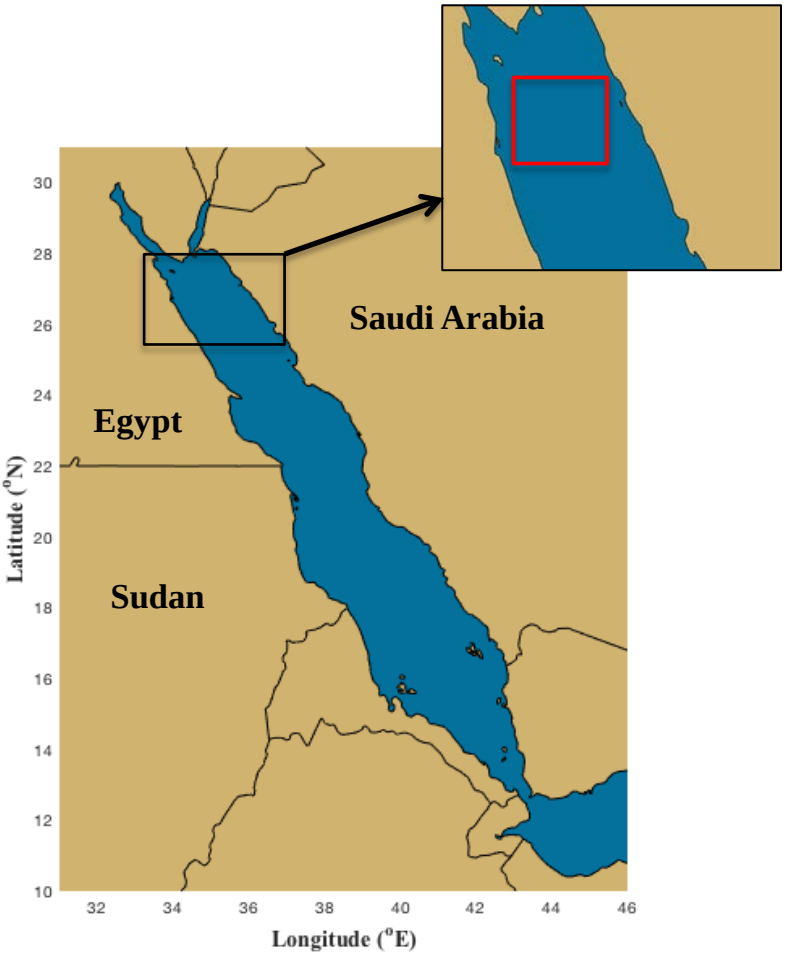

Figure. 1. Map displaying the geographical location of the NRS province (shown by the black box). Red box in the central NRS represents the area used for the extraction of vertical temperature profiles from the MIT general circulation model.

2.2 Satellite ocean-colour data

Version 3 of the Ocean Colour Climate Change Initiative (OC-CCI) product, developed by the European Space Agency [Sathyendranath *et al.*, 2016], was used in this study. This product consists of merged and bias-corrected Chl-a data from the SeaWiFS, MODIS, MERIS and VIIRS satellite sensors. Level 3 mapped data were acquired at 4 km and 8-day resolutions from http://www.esa-oceancolour-cci.org.

The OC-CCI product is developed as follows: data from the different satellite instruments are merged after band shifting and bias correction to allow consistency between sensors, and then error characterised based on validation with global *in situ* data. The POLYMER atmospheric correction algorithm is used for processing data from the MODIS and MERIS, which improves the retrieval of ocean colour data under adverse conditions such as sun glint, thin cloud cover and high aerosol optical depths [Steinmetz *et al*., 2011]. For processing SeaWiFS and VIIRS data, the SeaDAS atmospheric correction is used [Fu *et al*., 1998]. Due to this multi-sensor approach, the OC-CCI dataset provides significantly improved coverage in comparison to other satellite datasets [Brewin *et al*., 2015; Racault *et al*., 2015] and is the most consistent time series of ocean colour data so far. Despite overall improved coverage, the time series may still contain outliers due to reduced data coverage during specific 8-day periods. Based on visual observation, outliers were removed from the Chl-a time series prior to analysis.

2.3 Estimation of phytoplankton phenology

The phenology of the winter phytoplankton bloom in the NRS was estimated using the threshold criterion method adopted by Racault *et al*. [2015] for their study of phytoplankton phenology in Red Sea coral reef ecosystems. The threshold criterion method is based on the concept that the occurrence of a phytoplankton bloom should correspond to a significant increase in biomass above normal concentrations [Siegel *et al*., 2002]. The method can be briefly summarized as follows: First, the seasonal climatology of Chl-a was generated using the OC-CCI 8-day Chl-a data, spatially averaged over the study region (see section 2.2). A threshold criterion of median + 5% was then calculated using the seasonal climatology. Chl-a anomalies were computed by subtracting the threshold criterion from the climatology time series and the cumulative sums of Chl-a anomalies was generated. An increasing (decreasing) trend in the cumulative sums of anomalies time series represents periods when Chl-a concentrations are above (below) the threshold criterion. Finally, the derivative of the cumulative sums of anomalies was computed to identify the transition points between increasing and decreasing trends. Phenological indices (the timing of bloom initiation and termination) corresponded to the 8-day periods when the derivative was equal to zero (i.e. when Chl-a concentrations first rose above and below the threshold criterion). The duration corresponded to the period between initiation and termination. The reader is referred to Racault *et al*. [2015] (their Figure. 1) for further information regarding this methodology.

For calculating interannual phenological indices, the median of the entire time series was computed and the same threshold criterion (median + 5%) was utilized to

determine the timings of initiation, termination and duration for every year (see methodology above). The anomalies of the phenological indices were simply calculated by subtracting each index from the overall mean.

2.4. Sea surface temperature data

A level 4, gap-free, blended sea surface temperature (SST) dataset (GHRSST AVHRR_OI), downloaded from https://podaac.jpl.nasa.gov, was used to investigate the relationship between Chl-a and temperature. This global SST product utilises data obtained from the Advanced Very High Resolution Radiometer (AVHRR) Pathfinder (version 5) time series, combined with *in situ* ship and buoy observations. Data were acquired at a daily temporal resolution and mapped on a grid with a spatial resolution of 0.25° by 0.25°. Daily data were averaged over the NRS to provide 8-day averages (see definition of NRS in section 2.1).

2.5 Model data

Outputs acquired from the high resolution (~1.8 km) MIT general circulation ocean model (MITgcm), specifically designed to study the general circulation of the Red Sea [Yao *et al*., 2014], were used to generate the vertical profiles of temperature in the NRS, The model covers the entire Red Sea and was forced with reanalysis atmospheric data from the National Centers for Environmental Prediction (NCEP) [Kalnay *et al*., 1996; Stephens *et al*., 2002; Yao *et al*., 2014]. It has successfully been used to describe the overturning circulation in the Red Sea and was further used for analysing the seasonal

variability of the energetic mesoscale activity of the basin [Zhan *et al*., 2014]. To represent the overall temperature profile of the NRS, mean profiles were extracted from a region in the central NRS (red box, Fig. 1). Estimations of the mean mixed layer depth (MLD) were performed using a temperature-difference based criteria. Commonly used values lie in the range of 0.01-1.0°C for potential temperature [Dong *et al*., 2008]. For this study, a threshold value of 0.125°C was chosen.

Modeled outputs of heat flux were acquired from a high resolution (10 km), assimilated atmospheric product, developed at KAUST using the Advanced Research – Weather Research and Forecasting atmospheric model [Viswanadhapalli *et al*., 2016; Skamarock *et al*., 2005]. The model simulations were performed on a two-way nested domain (30 km and 10 km resolution) that covers the Red Sea and its adjacent regions. Initial and boundary conditions were acquired from the NCEP Final Analysis product. Comparisons with *in situ* and other gridded data products have shown that this assimilated product successfully reproduces spatiotemporal patterns of wind, temperature and sea level pressure over the Red Sea [Viswanadhapalli *et al*., 2016]

3. RESULTS

3.1 Phytoplankton phenology in the Northern Red Sea

Based on 18 years of Chl-a and SST data, a climatology was generated to show the general phytoplankton phenology in the NRS. The analysis reveals that the bloom initiates in mid-November, terminates in mid-April and has an overall duration of ~ 5 months (Fig. 2). Overall, highest Chl-a concentrations (~ 0. 27 mg/m^3) can be detected in the NRS at the beginning of February and subsist until mid-March, representing the average peak of the bloom. During this period, Chl-a concentrations remain high and are generally stable. Lowest SST in the region occurs at approximately the same time and begins to increase at the start of April, corresponding to a decrease in Chl-a. Chl-a concentrations reach a minimum of ~ 0.14 mg/m^3 during summer (July – September), coinciding with the seasonal increase in SST due to overall warmer atmospheric conditions over the Red Sea.

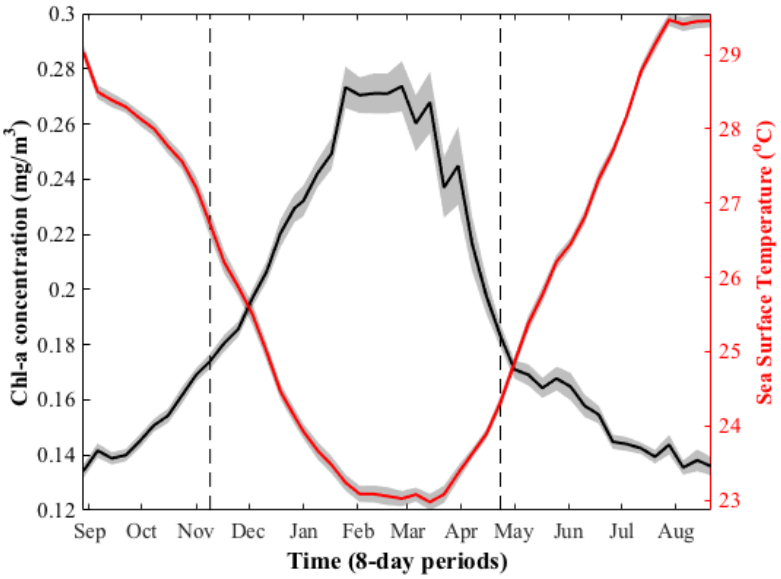

Figure. 2 Seasonal climatology of the Chl-a and SST area mean over the NRS (black line and red line respectively), averaged over the period 1998-2015. Dashed vertical lines represent the timing of bloom initiation and termination. Shaded areas surrounding each line represent the values +/- the standard error

3.2 Interannual variability of Chl-a and SST

To investigate the relationship between Chl-a concentrations and SST at an interannual scale, the two parameters, averaged over the NRS, and their respective anomalies were plotted for the full period (1998-2015) and are presented in Figure 3. Overall it is apparent that the time series is dominated by seasonal variability, with the highest values occurring during the winter-spring period (Fig. 3a). In 2007, 2008 and 2012, Chl-a anomalies are relatively high (0.05 – 0.08 mg/m^3) and remain elevated throughout the whole duration of the bloom period, co-occurring with colder SSTs (Fig. 3b). Large peaks can be observed in specific years in the Chl-a time series (e.g. 2000, 2001, 2003 and 2012) when concentrations have reached > 0.4 mg/m^3 during the blooming period (Fig. 3a). In 2000, 2001 and 2003, Chl-a anomalies during the bloom (grey shaded bars) are between ~ 0.1 and 0.2 mg/m^3 higher than the average concentrations for a period of ~ 1-2 weeks (Fig. 3b). Chl-a concentrations reach a maximum of only ~ 0.24 mg/m^3 during the blooming periods of 1998, 1999, 2009 and 2010. In the case of 1999 and 2010, this co-occurs with notably warmer winter SSTs (Fig. 3a). This can be observed clearly in the anomalies, where Chl-a concentrations are 0.08 - 0.10 mg/m^3 lower than usual in the winters of 1999 and 2010, and correspond to SSTs that are 0.1 and 0.2°C warmer, respectively (Fig. 3b). Warmer conditions during blooming periods and reduced Chl-a concentrations are also apparent in 2013 and 2014, although to a lesser extent.

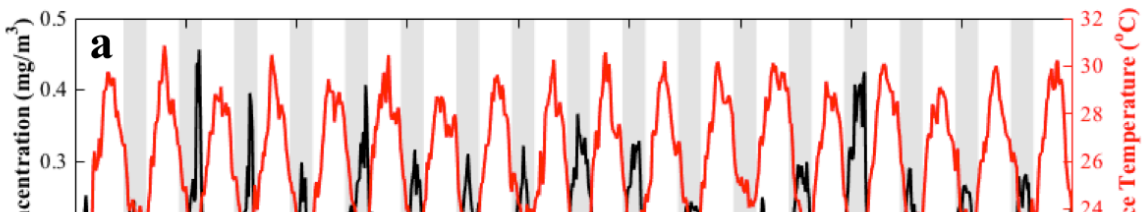

Figure. 3 a) Time series (8-day averages) of Chl-a concentration (mg/m^3) and SST (°C) in the NRS for the period 1998-2015. Grey shaded bars represent the overall blooming period (mid-Nov to mid-Apr) based on the seasonal analysis of phytoplankton phenology. **b)** Corresponding anomalies (climatological mean for each 8-day period minus absolute values) for Chl-a and SST in the NRS.

To investigate this relationship further, and isolate the period that is likely of most ecological importance, the period representing the peak of the bloom (February-March based on the general phenology, Fig. 2) was isolated and plotted interannually with SST. There is a significant negative relationship (ρ = - 0.75, p = 0.0008) between Chl-a and SST during the peak of the bloom is (Fig. 4). The warmest SSTs occur in 1999 and 2010 (~ SST is 0.75°C and 1.5°C above the mean respectively), coinciding with the weakest bloom peaks throughout the 17-year period (Chl-a concentrations 0.07 - 0.08 mg/m^3 below average). Intense blooms in 2007 and 2012 parallel SSTs that are ~ 0.5 degrees cooler than normal.

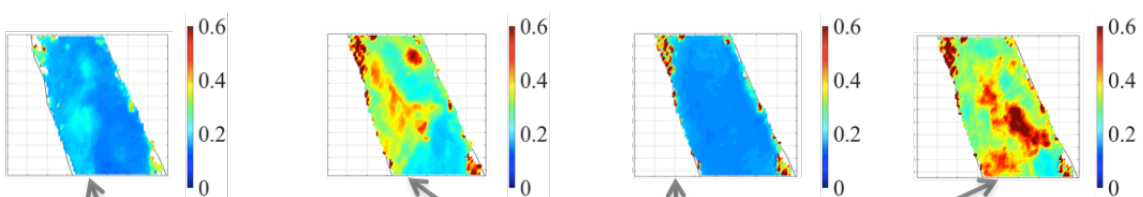

Figure 4. Annual time series of Chl-a (black line) and SST anomalies (red line) during the peak of the phytoplankton bloom period (February – mid-March). Red and grey shaded bars represent the two 'extreme' years when Chl-a is highest (2007 and 2012) and lowest (1999 and 2010) in the NRS. Spatial maps of Chl-a (four upper panels) and SST (four lower panels) are presented for these corresponding years.

3.3 Relationship between Chl-a, MLD and winter heat flux

To explore the physical mechanisms associated with interannual changes in Chl-a concentrations, datasets of monthly vertical water temperature, MLD and Chl-a anomalies were analysed. Strong positive Chl-a anomalies during the winters of 2000, 2003, 2007 and 2012, co-occur with a deeper MLD and colder temperatures (21.5^{o}C, Fig. 5a), which extend all the way to the surface. The monthly anomalies of Chl-a and MLD correlate significantly (r = 0.3, p = 0.00004, Fig. 5b). The MLD is deepest (~ 275 metres) in the winter of 2007. The winters of 1999 and 2010 are characterised by a substantially shallower MLD (~ 50 metres shallower than the mean, Fig. 5b), co-occurring with anomalously low Chl-a concentrations (- 0.05 mg/m^3) and warmer temperatures in the upper 75 metres (Fig. 5a). Higher Chl-a anomalies also occur in 2003, when the MLD is 50 metres shallower than average.

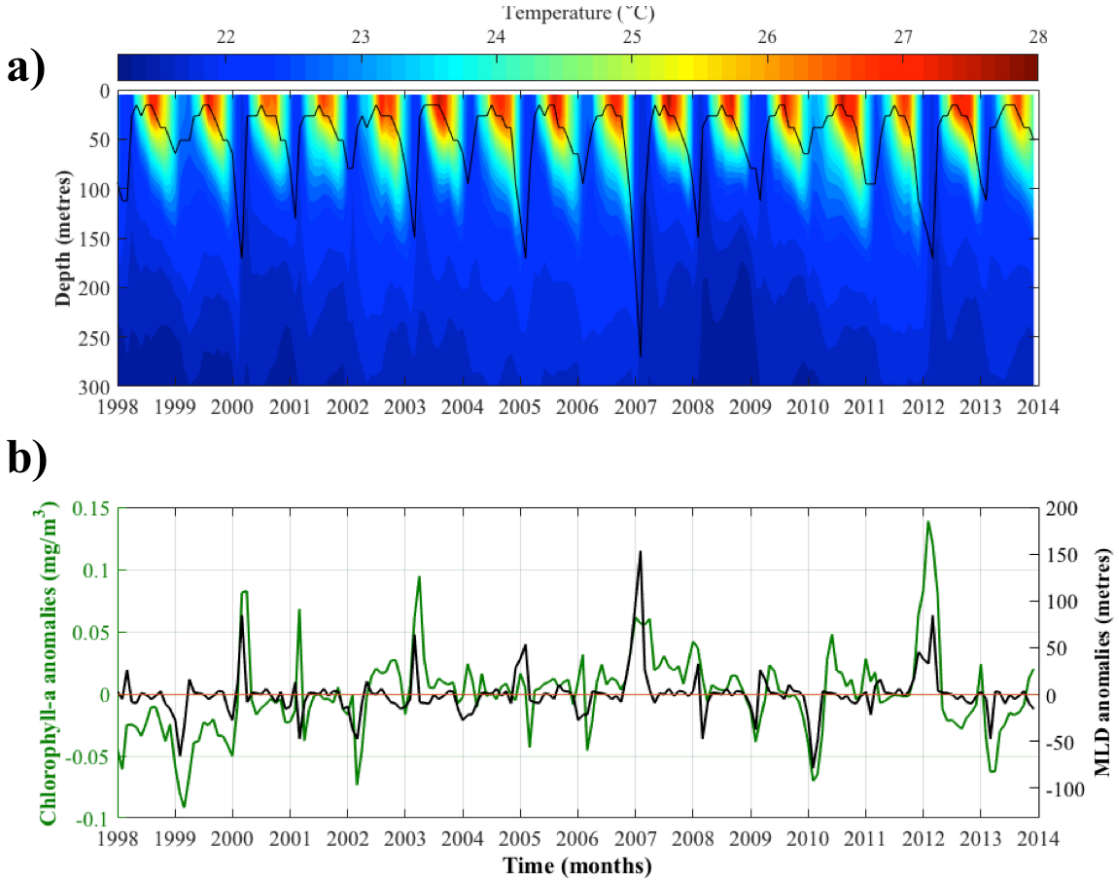

Figure 5. a) Contour plot displaying vertical temperature profiles (box-area averaged, Fig.1) in the central NRS for the period 1998-2014. Overlaid black line represents the average monthly MLD. **b)** Monthly time series of Chl-a and MLD anomalies (metres) for the same period.

The atmospheric link between vertical mixing and Chl-a interannual variability was also explored by investigating the relationship between the anomalies of winter (November – March) upward heat flux and the annual Chl-a anomalies. A significant positive correlation is apparent between the two variables ($\rho = 0.64$, $p < 0.05$, Fig. 6).

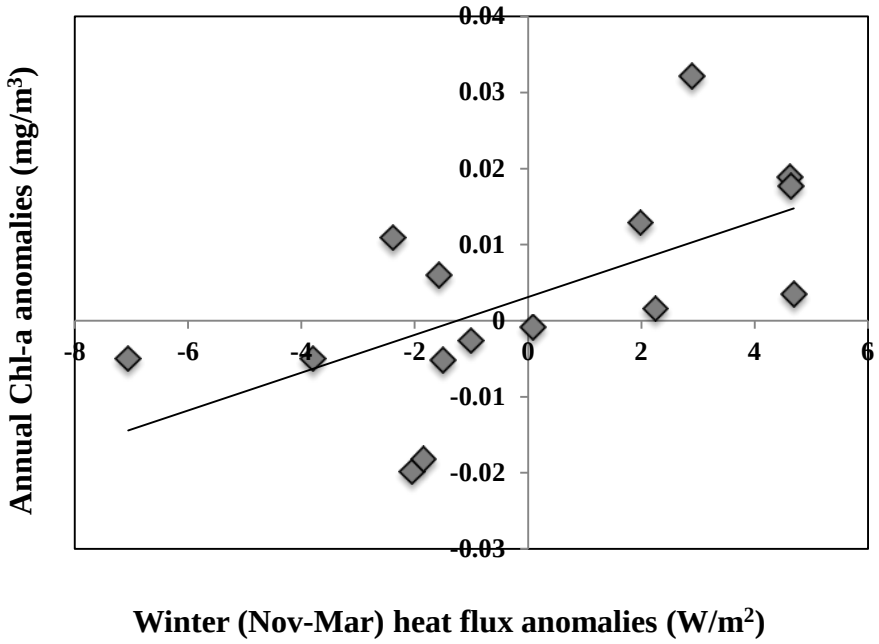

Figure 6. Scatterplot of relationship between annual Chl-a anomalies (mg/m^3) and the winter (November-March) anomalies of upward heat flux (W/m^2).

3.4 Interannual variability of phenological indices

To investigate whether years that are characterised by low/high Chl-a concentrations also represent a change in bloom timing, the anomalies of annual Chl-a concentrations and phenological indices (initiation, duration and termination) are presented in Figure 7. The

initiation of the bloom occurs significantly later (ρ = -0.55, $p < 0.05$) during years when annual Chl-a concentrations are reduced (Fig. 7d). For instance, the bloom of 1999, the second warmest year in the time series, Fig. 4) occurs ~ 4 weeks later than average (Fig. 7a). The most delayed (+ 6.5 weeks) initiation occurs in 2000. Low Chl-a concentrations in 2013 correspond to a bloom that initiates ~ 2.5 weeks later. In 2007 and 2012 (the strongest bloom peaks, Fig. 4), the bloom initiates ~ 1.5 weeks earlier, whilst the earliest initiation (~ 4.5 weeks) occurs in 2003 when annual chlorophyll-a concentrations are ~ 0.02 mg/m^3 higher than the 17-year mean (Fig. 7a). Longer bloom duration parallels higher Chl-a concentrations significantly (ρ = 0.51, $p < 0.05$) and the duration may be ~ 1 - 8 weeks longer than average, depending on the year (Fig. 7b, e). Conversely, when Chl-a is significantly reduced (1999, 2013 and 2014) the bloom may be 3-10 weeks shorter. Bloom termination is strongly positively correlated with annual Chl-a concentrations (ρ = 0.41, $p > 0.05$, Fig. 7c, f). Termination occurs ~ 4 - 8 weeks earlier during periods years of low Chl-a. The earliest bloom terminations (- 4 - 8 weeks) occur in 1999, 2013 and 2014.

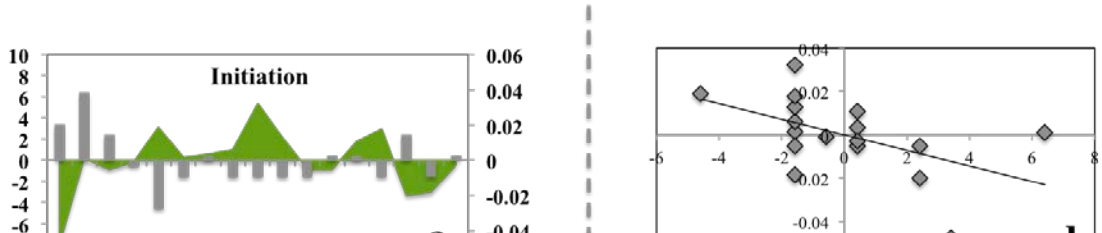

Figure 7. (a-c) Time series of annual Chl-a anomalies (mg/m^3) in the NRS (represented by the green-shaded area) plotted against the anomalies (in weeks) of bloom initiation, duration and termination (grey vertical bars). **(d-f)** Scatterplots displaying Chl-a anomalies plotted against phenology anomalies.

3.5. Physical controls on phytoplankton phenology

The results so far clearly show that absolute values of Chl-a are lower during warmer years. However, this gives no information regarding the influence of a warmer environmental state on the timing of phytoplankton availability. Thus, relationships between phytoplankton phenology and the regional physical environment were investigated. Significant relationships are only observed between the phenological metrics and winter (November-March) upward heat flux (Fig. 8). Winter upward heat

flux is positively correlated with the anomalies of duration (ρ = 0.55, p < 0.05) and termination (ρ = 0.44, p > 0.05) and strongly negatively correlated with initiation (ρ = -0.56, p < 0.05).

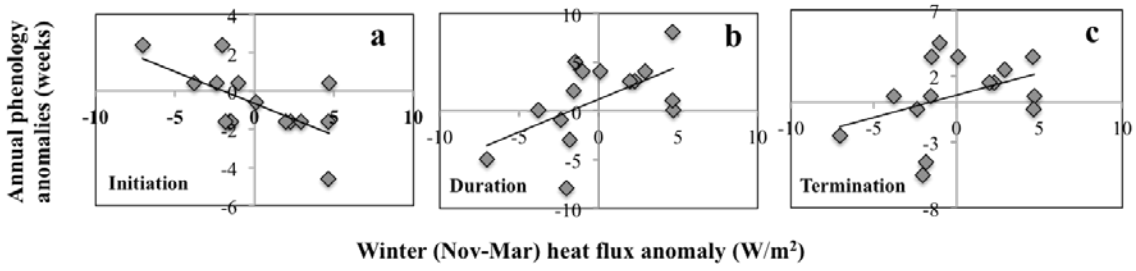

Figure 8. Scatterplots of winter (Nov-Mar) heat flux anomalies (W/m^2) vs. annual anomalies of **(a)** bloom initiation **(b)** bloom duration **(c)** bloom termination

4. DISCUSSION

4.1 Interannual variability of Chl-a concentrations

The analysis of phytoplankton phenology (initiation in November, peak in February-March and termination in April) is consistent with the findings of Racault *et al.* [2015], who computed phytoplankton phenology for a small region in the central NRS (Fig. 2). Due to the oligotrophic nature of the NRS and the lack of nutrient input from other sources (e.g. rivers, land run-off), phytoplankton seasonality is strongly coupled with the seasonal cycle of SST, suggesting that the annual occurrence of the NRS winter bloom is dependent on the vertical mixing of nutrients from colder, deep layers, across the pycnocline, and into the euphotic layer [Sofianos and Johns, 2003; Acker *et al*., 2008 Raitsos *et al*., 2013; Triantafyllou *et al*., 2014]. We found that the average duration of the bloom is 5 months, although the physical regime in the NRS can generate phytoplankton growth periods that may endure for up to 6 months [Racault *et al*., 2015].

The interannual variability of Chl-a concentrations in the NRS appears to be controlled by the variability of vertical mixing (Fig. 5). Based on SST, the warmest years during the bloom occur in 1999 and 2010 (Fig. 3 & 4). These years are characterised by a shallow MLD (~ 50 metres), which co-occurs with reduced Chl-a concentrations and warmer temperatures in the first 50 – 100 m (Fig. 5). In this type of physical regime, stratified conditions inhibit the replenishment of nutrients in the euphotic zone, ultimately contributing to diminished phytoplankton productivity. Indeed, by using a model-based approach, Behrenfeld *et al*. (2006) demonstrated that a reduction in net primary

productivity in the stratified oceans at the interannual level is linked to the intensification of water column stratification. It is worth mentioning that highest SSTs in the winter of 2010 (1.5°C higher than average during the peak of the bloom, Fig. 4) are likely related to an El Niño event that occurred during this year [Kim *et al*., 2011]. Positive phases of the El Niño Southern Oscillation have been correlated with enhanced stratification, a deeper nutricline and reduced Chl-a concentrations in other tropical regions such as the Equatorial Pacific Ocean [Behrenfeld *et al., 2006*, Martinez *et al*., 2009]. Colder years as shown by SST (e.g. 2007 and 2012) represent a deepening of the mixed layer (increased mixing within the water column) and increased nutrient transport to the surface layers.

SST in the NRS is an effective indicator of vertical mixing. However, the holistic mechanism that drives vertical mixing, and ultimately controls the interannual variability of Chl-a concentrations is better represented by the winter net air-sea heat exchange (heat flux, Fig. 6). Collectively, total heat flux is the sum of shortwave radiation (solar), longwave radiation (infrared), latent heat (evaporative) and sensible heat (air-sea temperature difference). Heat exchanges with the atmosphere modulate the warming and cooling of the sea surface [Papadopoulos *et al*., 2013] and drives convection (mixing) processes that redistribute nutrients from deeper layers to the surface. Winter (November-March) heat flux showed a stronger correlation with annual Chl-a concentrations in comparison to SST (results not shown). This can potentially be explained by considering other mechanisms that may have an influence on SST, which are not necessarily linked to vertical mixing. For example, SST has been shown to also depend on the general cyclonic circulation in the NRS [Papadopoulos *et al.*, 2015], the vigorous and highly variable eddy activity [Zhan *et al*., 2014] and the lateral advection of water masses from neighboring

regions following the general Red Sea circulation.

In general, it appears that colder years are linked with increased air-sea heat exchange, stronger convection events and an increase in nutrient availability. Conversely, warmer years are associated with a reduction in heat fluxes, relatively stronger stratification and therefore reduced nutrient transport from deeper layers. This ultimately leads to lower phytoplankton abundance in the NRS. Indeed, a direct relationship between lower surface heat losses to the atmosphere and weaker phytoplankton blooms at an interannual scale has been documented in the Southern Adriatic Sea by Gačić *et al*. [2002].

It is important to note that other physical factors may contribute to the transport of nutrients to the surface layer. For example, highest Chl-a concentrations during the bloom period occur in 2012 (Fig. 3, Fig. 4), but do not coincide with the deepest MLD (2007, Fig. 5) or the coolest SST (2008, Fig. 3, Fig. 4). This is generally consistent with the analysis of Papadopoulos *et al*. [2015] who revealed that vertical transport of nutrients can also be induced by the permanent cyclonic circulation which is present between 26°N and 27°N in the NRS [Morcos, 1970; Clifford *et al*., 1997; Sofianos and Johns, 2003]. The formation and intensification of cyclonic gyres is known to induce a flux of nutrients from deeper waters to the surface layer [McGillicuddy and Robinson, 1997; McGillicuddy, 2016]. Papadopoulos *et al*. [2015] demonstrated that the activity of the gyre varies interannually. Specifically, the authors showed that the gyre is more active throughout 2011, meaning that persistent upwelling associated with the gyre prior to the winter of 2012 contributes to elevated concentrations of nutrients in the region. Thus, at the timing of bloom initiation in November 2012, ample levels of nutrients in the NRS

likely contribute to the highest levels of phytoplankton biomass observed in this year.

Significant deepening of the MLD in 2007 may also be attributed to increased cyclonic gyre activity in the NRS (Fig. 5a, 5b). The occurrence of the deepest MLD in 2007 would intuitively suggest that coldest SST's are apparent during this year. However, in this study, minimum SST is observed in 2008 (Fig. 3a). Papadopoulos *et al*. [2015] revealed that the gyre is more active in the autumn of 2006, prior to the initiation of the 2007 winter bloom. Thus, this preconditioning (upwelling of colder waters) and the presence of colder conditions at the start of the winter in 2007 likely contribute to more intense vertical mixing and a significant deepening of the mixed layer.

4.2 Interannual variability of phytoplankton phenology

At an interannual level, Chl-a concentrations were significantly correlated with the initiation and duration of the bloom (Fig. 7d, e). In other words, during warm years, lower Chl-a concentrations were related to a bloom that initiated later and was shorter in duration, whilst the opposite relationship was detected for cold years. This contrasts to what has been observed in other studies. For instance, in a global study of phytoplankton phenology, Racault *et al*. [2012] observed that, for low productivity regions, positive anomalies of bloom duration occur during years when phytoplankton biomass remains low, which was attributed to the low seasonality of the region.

In the case of this study, the same physical mechanism appears to control both phytoplankton abundance and phenology. Analysis of several physical parameters revealed that heat flux averaged over the winter period (November-March) was the most

important parameter influencing phenological indices (Fig. 8). This can potentially be explained as follows: in warmer winters (reduced heat fluxes), more stratified conditions increase the amount of time that it takes for vertical mixing to reach an appropriate depth where nutrients are abundant and thus can be transported to the surface layers. Similarly, a decrease in the intensity of mixing, combined with a later initiation is likely to result in blooms that have a shorter duration. Conversely, during colder winters (characterised by stronger heat fluxes), convection events and the subsequent deepening of the mixed layer are likely to take place earlier, contributing to an earlier bloom initiation. Prolonged colder periods throughout winter may also contribute to more intense mixing and extend the duration of the bloom.

Although the general relationship between phytoplankton phenology and the regional physical environment is clear, some variability is apparent. In some years, although annual Chl-a anomalies are similar, notable differences in the initiation of the bloom can be detected (e.g. 2003 and 2007, Fig. 7a). For some years, it is possible that the mixed layer reaches significantly deeper depths, where nutrients are abundant, resulting in large nutrient fluxes to the surface and overall high Chl-a concentrations. In other years, although the mixed layer may not penetrate as deeply, it may reach depths where nutrient levels are just adequate enough to stimulate a phytoplankton bloom earlier, resulting in lower Chl-a concentrations overall, but an earlier bloom initiation. In addition, fluctuations in the intensity and frequency of heat losses to the atmosphere could also explain the variability in the duration of the bloom during years when similar Chl-a concentrations can be observed (e.g. 2003 and 2012, Fig. 7b). For instance, high heat flux events during winter may occur in short, intense bursts, contributing to high

Chl-a concentrations due to short ‘pulses’ of nutrients to the surface, but shorter bloom duration. Alternatively, periods when air-sea heat exchange is more gradual may increase Chl-a concentrations to the same level, but over a longer time period, causing longer bloom duration.

Annual Chl-a concentrations are highest in 2007 (Fig. 7), and yet coincide with an initiation that is just 2 weeks earlier, a duration which is 4 weeks longer and a termination date which is 2 weeks later (Fig. 7a, b, c). Similarly, the winter net flux anomaly in 2012 was among the highest over the last 17 years (results not shown), and yet the response observed in phytoplankton phenology is relatively minimal. Thus, it is possible that other factors may regulate bloom timing. The impact of zooplankton grazing on phytoplankton is not yet well understood in the Red Sea, and it is possible that enhanced grazing during years of high productivity may exert a control on bloom timing. Sommer *et al*. [2002] demonstrated that grazing by microzooplankton and appendicularians in the NRS between February and March is an important control on algal biomass. However, further work is needed to assess the impact of grazing on phytoplankton phenology.

4.3 Potential biological implications of Northern Red Sea warming

Tropical SSTs are predicted to rise by up to 3°C in this century [Mcleod *et al*., 2016; Ganachaud *et al*., 2011; Meehl *et al*., 2007] and an abrupt increase in SST across the Red Sea has been documented by Raitsos *et al*. [2011]. Building upon these findings, analysis of both sea surface temperature and the average upper water column temperature (first 300 metres) revealed that the NRS has been warming over the last three decades (Fig. 9).

Years characterised by warmer conditions (reduced heat losses to the atmosphere), which do not favour vertical mixing over the NRS, are associated with an overall reduction Chl-a concentration (phytoplankton biomass), due to depleted levels of nutrients in the water column. In coral reef ecosystems, phytoplankton is a direct food source for sponges [Richter *et al*., 2001], bi-valves [Yahel *et al*., 2009] and pelagic larvae [Erez, 1990; Lo-Yat *et al*., 2011]. Consequently, a reduction in food availability may have direct ramifications for higher trophic levels in the NRS. Indeed, Lo-Yat *et al*. [2011] demonstrated that elevated water temperature in the reefs of French Polynesia was significantly related to a reduction in Chl-a concentrations, which in turn was linked to a 50% reduction in fish larval supply to the reef due to increased larval mortality. Furthermore, in response to a decrease in food availability during warmer El Niño conditions, slower growth rates of three herbivorous damselfishes has been observed in the coral reefs of the Galapagos islands [Meekan *et al*., 1999; Munday *et al*., 2008].

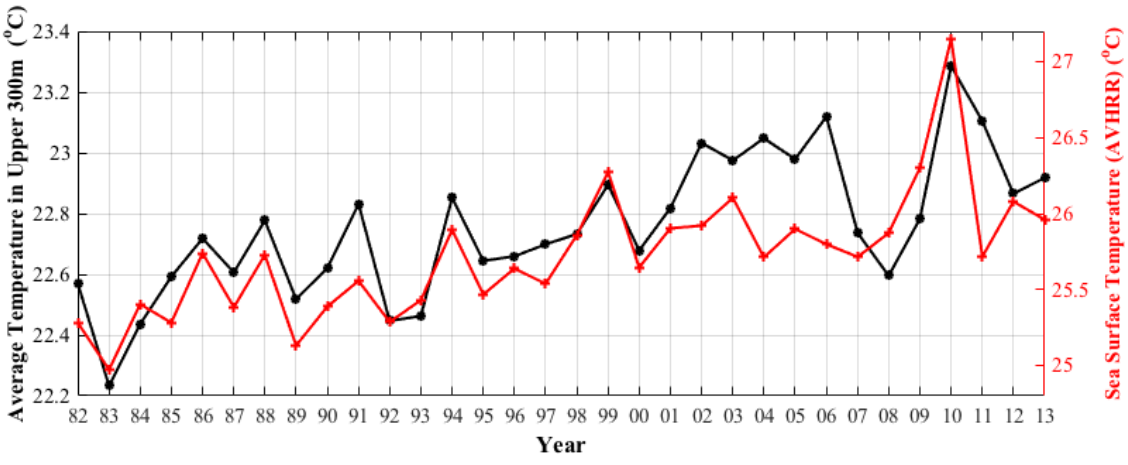

Figure. 9. Time series of annual AVHRR SST averaged across the whole NRS (red line) and the average temperature of the upper 300 metres of the water column in the central NRS (box-averaged [see Fig.1] temperature values based on modeled outputs from MITgcm).

Aside from an overall decrease in phytoplankton biomass, warmer winters are significantly associated with a change in phytoplankton phenology in the NRS. This analysis revealed that reduced upward heat fluxes during winter are significantly correlated with an earlier phytoplankton bloom initiation and shorter bloom duration. Subsequent alterations in phytoplankton seasonality may have far-reaching consequences for higher trophic levels due to the mismatch between the timing of food availability (phytoplankton) and the presence of planktonic larvae [Cushing, 1972, 1990].

The reproductive strategies of reef species may be impacted by changes in phenology. The spawning of some species of herbivorous reef fishes in the Red Sea (Gulf of Aqaba) during summer may be associated with the deterioration of body condition due to increased energy expenditure on gonadal elaboration [Montgomery *et al.,* 1989]. Body condition of these species was shown to increase during the winter months, coinciding with the occurrence of benthic green algal blooms in the Gulf of Aqaba due to winter vertical mixing and increased nutrient supply. Metabolic requirements are only likely to be sufficiently met during this period, and it has been shown that increased winter-feeding provides support for subsequent reproductive events [Montgomery *et al*., 1989]. Although the Gulf of Aqaba was not incorporated into the analysis of this study, earlier bloom initiation due to warming (and increased stratification), and the decoupling of food availability may ultimately impact the fitness and reproductive output of herbivorous reef fish.

Under a scenario of warmer conditions in the NRS, delayed initiation of the winter bloom seems likely. A decline in the recruitment of larval fish may occur if the initiation of the bloom begins to occur later in the year, and the spawning of larval fish

continues to match the original timing of bloom initiation prior to warming [Cole, 2013]. If the recruitment of a commercially important fish species is negatively impacted, there may be unprecedented consequences for coastal populations that depend on fisheries resources for sustenance and their economy. Indeed, this has been observed in the North Sea where an increase in sea surface temperature altered the planktonic component of the marine food web, causing a decrease in the recruitment of Atlantic cod (*Gadhus morhua*) [Beaugrand *et al*., 2003].

This study supports the hypothesis that warmer conditions in the NRS will lead to an alteration in phytoplankton bloom timing. However, it is worth noting that an increase in temperature may have indirect impacts on marine organisms. Studies have shown that reef fish may exhibit shorter larval durations in response to rising temperatures [Green and Fisher, 2004; Sponaugle *et al.*, 2007]. Consequently, the combined impact of a significant delay in bloom initiation, and shorter larval duration, may exacerbate the mismatch between food availability and reef fish larvae. In addition, warmer conditions may be linked to an exponential increase in the metabolic activity of ectotherms [Gillooly *et al*., 2001; Dillon *et al*., 2010]. An increase in metabolic rate during anomalously warm years may increase the energy requirements of organisms that are already living under conditions of reduced food availability, contributing to higher mortality rates.

Finally, future phenological shifts could be related to a change in the community structure of phytoplankton as a result of increasingly warm conditions. The dominant phytoplankton group in the NRS during winter is diatoms [Ismael, 2015]. Previous research has shown that an increase in nutrient-depleted conditions in the surface layer of the oceans will lead to the replacement of diatoms with smaller phytoplankton size

classes [Bopp *et al*., 2005]. This may subsequently lead to changes in phenology due to the different life strategies of the species.

5. CONCLUSIONS

Using a combination of remotely-sensed Chl-a and SST, as well as modeled outputs of vertical temperature profiles, mixed layer depth and heat flux, this study investigated the long-term interannual variability of phytoplankton biomass and phytoplankton phenology in the NRS, in relation to the regional physical environment.

The overall phenology of NRS phytoplankton was identified and the blooming period was generally shown to initiate in mid-November, peak between February-March, and terminate in mid-April. Chl-a concentrations during the NRS winter bloom are strongly correlated with SST, which was shown to be a sensitive indicator for the intensity of vertical mixing. Vertical mixing in the NRS is ultimately controlled by winter net surface heat loss (heat flux), which drives convection events that redistribute cold, nutrient-rich waters from the deeper layers into the euphotic zone. Significantly reduced Chl-a concentrations were apparent during warm years, and this was attributed to a reduction in winter net surface heat loss (heat flux) and more persistent water column stratification, contributing to diminished nutrient availability.

Chl-a concentrations exhibited a significant relationship with phytoplankton phenology indices, indicating that bloom timing is affected by similar physical mechanisms. Specifically, the timing of bloom initiation and the overall duration were correlated with winter heat flux. During warm years, the timing of bloom initiation is delayed, which can be attributed to an increase in the amount of time needed for enough heat loss to generate enough mixing to break down stratified conditions. A reduction in the intensity of mixing also likely contributes to shorter bloom duration.

In light of these results, further warming in the NRS may have profound biological implications. Abrupt changes in phytoplankton phenology may result in the decoupling of pelagic larvae from their food source, increasing mortality rates, whilst subsequent decreases in the recruitment of commercial species may impact fisheries yields, causing negative economic and societal impacts. However, considering the complexity of phytoplankton communities, as well as the potential influence of other factors (e.g. grazing), the results of this study are just the first step in understanding how Red Sea marine algae may respond to their changing environment.

REFERENCES

Acker, J., Leptoukh, G., Shen, S., Zhu, T., & Kempler, S. (2008). Remotely-sensed chlorophyll a observations of the northern Red Sea indicate seasonal variability and influence of coastal reefs. *Journal of marine systems*, *69*(3), 191-204.

Armbrust, E. V., Berges, J. A., Bowler, C., Green, B. R., Martinez, D., Putnam, N. H., Zhou, S., Allen, A. E., Apt, K. E., Bechner, M. and Brzezinski, M. A. (2004). The genome of the diatom Thalassiosira pseudonana: ecology, evolution, and metabolism. *Science*, *306*(5693), 79-86.

Behrenfeld, M. J., O'Malley, R. T., Siegel, D. A., McClain, C. R., Sarmiento, J. L., Feldman, G. C., Milligan, A. J., Falkowski, P. G., Letelier, R. M. & Boss, E. S. (2006). Climate-driven trends in contemporary ocean productivity. *Nature*, *444*(7120), 752-755.

Beaugrand, G., Brander, K. M., Lindley, J. A., Souissi, S., & Reid, P. C. (2003). Plankton effect on cod recruitment in the North Sea. *Nature*, *426*(6967), 661-664.

Berumen, M. L., Hoey, A. S., Bass, W. H., Bouwmeester, J., Catania, D., Cochran, J. E., Khalil, M. T., Miyake, S., Mughal, M. R., Spaet, J. L. Y. & Saenz-Agudelo, P. (2013). The status of coral reef ecology research in the Red Sea. *Coral Reefs*, *32*(3), 737-748.

Bopp, L., Aumont, O., Cadule, P., Alvain, S., & Gehlen, M. (2005). Response of diatoms

distribution to global warming and potential implications: A global model study. *Geophysical Research Letters*, *32*(19).

Brewin, R. J. W., Raitsos, D.E., Dall'Olmo, G., Zarokanellos, N., Jackson, T., Racault, M-F., Boss, E., Sathyendranath, S., Jones, B. H., & Hoteit, I. (2015). Regional ocean-colour chlorophyll algorithms for the Red Sea. *Remote Sensing of Environment*, *165*, 64-85, doi: 10.1016/j.rse.2015.04.024.

Cantin, N. E., Cohen, A. L., Karnauskas, K. B., Tarrant, A. M., & McCorkle, D. C. (2010). Ocean warming slows coral growth in the central Red Sea. *Science*, *329*(5989), 322-325.

Clifford, M., Horton, C., Schmitz, J., & Kantha, L. H. (1997). An oceanographic nowcast/forecast system for the Red Sea. *Journal of Geophysical Research: Oceans*, *102*(C11), 25101-25122.

Cole, H. S. (2014). *The natural variability and climate change response in phytoplankton phenology.* Doctoral dissertation, University of Southampton.

Cushing, D. H. (1972). The production cycle and the numbers of marine fish. In *Symp. Zool. Soc. Lond,* Vol. 29, pp. 213-232.

Cushing, D. H. (1974). The natural regulation of fish populations. *Sea fisheries research*, 399-412.

Cushing, D. H. (1990). Plankton production and year-class strength in fish populations: an update of the match/mismatch hypothesis. *Advances in Marine Biology*, *26*, 249-293.

Dillon, M. E., Wang, G., & Huey, R. B. (2010). Global metabolic impacts of recent climate warming. *Nature*, *467*(7316), 704-706.

Done, T. J. (1999). Coral community adaptability to environmental change at the scales of regions, reefs and reef zones. *American Zoologist*, *39*(1), 66-79.

Doney, S. C. (2006). Oceanography: Plankton in a warmer world. *Nature*, *444*(7120), 695-696.

Dong, S., Sprintall, J., Gille, S. T., & Talley, L. (2008). Southern Ocean mixed-layer depth from Argo float profiles. *Journal of Geophysical Research: Oceans*, *113*(C6).

Edwards, M., & Richardson, A. J. (2004). Impact of climate change on marine pelagic phenology and trophic mismatch. *Nature*, *430*(7002), 881-884.

Erez, J. (1990). On the importance of food sources in coral-reef ecosystems. *Ecosystems of the world*, *25*, 411-418.

Fu, G., Baith, K. S., & McClain, C. R. (1998). SeaDAS: The SeaWiFS data analysis system. In *Proceedings of the 4th Pacific Ocean remote sensing conference, Qingdao, China* (Vol. 2831, p. 7379).

Furby, K. A., Bouwmeester, J., & Berumen, M. L. (2013). Susceptibility of central Red Sea corals during a major bleaching event. *Coral Reefs*, *32*(2), 505-513.

Gačić, M., Civitarese, G., Miserocchi, S., Cardin, V., Crise, A., & Mauri, E. (2002). The open-ocean convection in the Southern Adriatic: a controlling mechanism of the spring phytoplankton bloom. *Continental Shelf Research*, *22*(14), 1897-1908.

Ganachaud, A. S., Sen Gupta, A., Orr, J. C., Wijffels, S. E., Ridgway, K. R., Hemer, M. A., Maes, C., Steinberg, C. R., Tribollet, A. D., Qiu, B. and Kruger, J. C. (2011). Observed and expected changes to the tropical Pacific Ocean. *Vulnerability of tropical Pacific fisheries and aquaculture to climate change. Secretariat of the Pacific Community, Noumea, New Caledonia*, 101-187.

Gillooly, J. F., Brown, J. H., West, G. B., Savage, V. M., & Charnov, E. L. (2001). Effects of size and temperature on metabolic rate. *science*, *293*(5538), 2248-2251.

Green, B. S., & Fisher, R. (2004). Temperature influences swimming speed, growth and

larval duration in coral reef fish larvae. *Journal of Experimental Marine Biology and Ecology*, *299*(1), 115-132.

Hallegraeff, G. M. (2010). Ocean climate change, phytoplankton community responses, and harmful algal blooms: a formidable predictive challenge1. *Journal of phycology*, *46*(2), 220-235.

Hoegh-Guldberg, O. (1999). Climate change, coral bleaching and the future of the world's coral reefs. *Marine and freshwater research*, *50*(8), 839-866.

Hurd, C. L., Harrison, P. J., Bischof, K. and Lobban, C. S. (2014), *Seaweed Ecology and Physiology*. 2nd ed. Cambridge, Cambridge University Press, 22-23.

Ismael, A. A. (2015). Phytoplankton of the Red Sea. In *The Red Sea*. Springer Berlin Heidelberg. pp. 567-583.

Kalnay, E., Kanamitsu, M., Kistler, R., Collins, W., Deaven, D., Gandin, L., Iredell, M., Saha, S., White, G., Woollen, J. & Zhu, Y., 1996. The NCEP/NCAR 40-year reanalysis project. *Bulletin of the American meteorological Society*, *77*(3), pp.437-471.

Kim, W., Yeh, S. W., Kim, J. H., Kug, J. S., & Kwon, M. (2011). The unique 2009–2010 El Niño event: A fast phase transition of warm pool El Niño to La Niña. *Geophysical Research Letters*, *38*(15).

Lo-Yat, A. , Simpson, S. D., Meekan, M., Lecchini, D., Martinez, E., & Galzin, R. (2011). Extreme climatic events reduce ocean productivity and larval supply in a tropical reef ecosystem. *Global Change Biology*, *17*(4), 1695-1702.

Martinez, E., Antoine, D., D'Ortenzio, F., & Gentili, B. (2009). Climate-driven basin-scale decadal oscillations of oceanic phytoplankton. *Science*, *326*(5957), 1253-1256.

McGillicuddy, D. J., & Robinson, A. R. (1997). Eddy-induced nutrient supply and new production in the Sargasso Sea. *Deep Sea Research Part I: Oceanographic Research Papers*, *44*(8), 1427-1450.

McGillicuddy Jr, D. J. (2016). Mechanisms of physical-biological-biogeochemical interaction at the oceanic mesoscale. *Marine Science*, *8*.

McLeod, I. M., Rummer, J. L., Clark, T. D., Jones, G. P., McCormick, M. I., Wenger, A. S., & Munday, P. L. (2013). Climate change and the performance of larval coral reef fishes: the interaction between temperature and food availability. *Conservation Physiology*, *1*(1), cot024.

Meehl, G. A., Stocker, T. F., Collins, W. D., Friedlingstein, P., Gaye, A. J., Gregory, J. M., Kitoh, A., Knutti, R., Murphy, J. M., Noda, A. and Raper, S. C. B. (2007). Global

climate projections Climate Change 2007: The Physical Science Basis: Fourth Assessment Report of the Intergovernmental Panel on Climate Change.

Meekan, M. G., Wellington, G. M., & Axe, L. (1999). El Nino-Southern Oscillation events produce checks in the otoliths of coral reef fishes in the Galápagos Archipelago. *Bulletin of Marine Science*, *64*(2), 383-390.

Montgomery, W. L., Myrberg, A. A., & Fishelson, L. (1989). Feeding ecology of surgeonfishes (Acanthuridae) in the northern Red Sea, with particular reference to *Acanthurus nigrofuscus* (Forsskål). *Journal of Experimental Marine Biology and Ecology*, *132*(3), 179-207.

Morcos, S. A. (1970). Physical and chemical oceanography of the Red Sea. *Oceanogr. Mar. Biol. Annu. Rev*, *8*(73), 202.

Munday, P. L., Jones, G. P., Pratchett, M. S., & Williams, A. J. (2008). Climate change and the future for coral reef fishes. *Fish and Fisheries*, *9*(3), 261-285.

Papadopoulos, V. P., Abualnaja, Y., Josey, S. A., Bower, A., Raitsos, D. E., Kontoyiannis, H. & Hoteit, I. (2013). Atmospheric forcing of the winter air–sea heat fluxes over the northern Red Sea. *Journal of Climate*, *26*(5), 1685-1701.

Papadopoulos, V. P., Zhan, P., Sofianos, S. S., Raitsos, D. E., Qurban, M., Abualnaja, Y., Bower, A., Kontoyiannis, H., Pavlidou, A., Asharaf, T. T. & Zarokanellos, N. (2015). Factors governing the deep ventilation of the Red Sea. *Journal of Geophysical Research: Oceans*, *120*(11), 7493-7505.

Platt, T., Fuentes-Yaco, C., & Frank, K. T. (2003). Marine ecology: spring algal bloom and larval fish survival. *Nature*, *423*(6938), 398-399.

Platt, T., & Sathyendranath, S. (2008). Ecological indicators for the pelagic zone of the ocean from remote sensing. *Remote Sensing of Environment*, *112*(8), 3426-3436.

Racault, M. F., Le Quéré, C., Buitenhuis, E., Sathyendranath, S., & Platt, T. (2012). Phytoplankton phenology in the global ocean. *Ecological Indicators*, *14*(1), 152-163.

Racault, M. F., Raitsos, D. E., Berumen, M. L., Brewin, R. J., Platt, T., Sathyendranath, S., & Hoteit, I. (2015). Phytoplankton phenology indices in coral reef ecosystems: application to ocean-color observations in the Red Sea. *Remote Sensing of Environment*, *160*, 222-234.

Raitsos, D. E., Hoteit, I., Prihartato, P. K., Chronis, T., Triantafyllou, G., & Abualnaja, Y. (2011). Abrupt warming of the Red Sea. *Geophysical Research Letters*, *38*(14).

Raitsos, D. E., Yi, X., Platt, T., Racault, M. F., Brewin, R. J., Pradhan, Y., Papadopoulos, V. P., Sathyendranath, S. and Hoteit, I. (2015). Monsoon oscillations regulate fertility of the Red Sea. *Geophysical Research Letters*, *42*(3), 855-862.

Raitsos, D. E., Pradhan, Y., Brewin, R. J., Stenchikov, G., & Hoteit, I. (2013). Remote sensing the phytoplankton seasonal succession of the Red Sea. *PLoS One*, *8*(6), e64909.

Richter, C., Wunsch, M., Rasheed, M., KoÈtter, I., & Badran, M. I. (2001). Endoscopic exploration of Red Sea coral reefs reveals dense populations of cavity-dwelling sponges. *Nature*, *413*(6857), 726-730.

Sathyendranath, S. and Platt, T. (1997), Analytic model of ocean colour. *Appl. Opt.*, *36*, 2620-2629.

Sathyendranath, S., Brewin, R. J. W., Brockmann, C., Brotas, V., Ciavatta, S., Chuprin, A., Couto, A. B., Doerffer, R., Dowell, M., Grant, M., Groom, S., Horseman, A., Jackson, T., Krasemann, H., Lavender, S., Martinez Vicente, V., Mélin, F., Moore, T. S., Müller, D., Regner, P., Roy, S., Steinmetz, F., Swinton, J., Taberner, M., Thompson, A., Valente, A., Zühlke, M., Brando, V. E., Feldman, G., Franz, B., Frouin, R., Gould, Jr, R. W., Hooker, S., Kahru, M., Mitchell, M. G., Muller-Karger, F., Sosik, H. M., Voss, K. J., Werdell, J., & Platt, T. (2016). Creating an ocean-colour time series for use in climate studies: the experience of the ocean-colour climate change initiative. *Remote Sensing of Environment*, Submitted.

Skamarock, W. C., Klemp, J. B., Dudhia, J., Gill, D. O., Barker, D. M., Wang, W., & Powers, J. G. (2005). *A description of the advanced research WRF version 2* (No. NCAR/TN-468+ STR). National Center For Atmospheric Research Boulder Co Mesoscale and Microscale Meteorology Div.

Sofianos, S. S., & Johns, W. E. (2003). An oceanic general circulation model (OGCM) investigation of the Red Sea circulation: 2. Three‐dimensional circulation in the Red Sea. *Journal of Geophysical Research: Oceans*, *108*(C3).

Solomon, S., Qin, D., Manning, M., Chen, Z., Marquis, M., Averyt, K. B., Tignor, M. & Miller, H.L. (2007). IPCC, 2007: Summary for Policymakers, Climate Change 2007: The Physical Science Basis. Contribution of Working Group I to the Fourth Assessment Report of the Intergovernmental Panel on Climate Change.

Sommer, U., Berninger, U. G., Böttger-Schnack, R., Hansen, T., Stibor, H., Schnack-Schiel, S. B., Cornils, A., Hagen, W., Wickham, S., Al-Najjar, T. & Post, A. F. (2002). Grazing during the spring bloom in the Gulf of Aqaba and the Northern Red Sea. *Marine Ecology Progress Series*, (239), 251-261.

Sponaugle, S., Grorud-Colvert, K., & Pinkard, D. (2006). Temperature-mediated variation in early life history traits and recruitment success of the coral reef fish Thalassoma bifasciatum in the Florida Keys. *Marine Ecology Progress Series*, *308*, 1-15.

Steinmetz, F., Deschamps, P. Y., & Ramon, D. (2011). Atmospheric correction in presence of sun glint: application to MERIS. *Optics express*, *19*(10), 9783-9800.

Stephens, C., Antonov, J. I., Boyer, T. P., Conkright, M. E., Locarnini, R. A., O'Brien, T. D., & Garcia, H. E. (2002). World Ocean Atlas 2001. Volume 1, Temperature.

Suzuki, R. and Ishimaru, T. (1990), An improved method for the determination of phytoplankton chlorophyll using N, N-dimethylformamide, *J. Oceanogr. Soc. Japan*, *46*(4), 190-194.

Triantafyllou, G., Yao, F., Petihakis, G., Tsiaras, K. P., Raitsos, D. E., & Hoteit, I. (2014). Exploring the Red Sea seasonal ecosystem functioning using a three‐dimensional biophysical model. *Journal of Geophysical Research: Oceans*, *119*(3), 1791-1811.

Winder, M., & Schindler, D. E. (2004). Climate change uncouples trophic interactions in an aquatic ecosystem. *Ecology*, *85*(8), 2100-2106.

Viswanadhapalli, Y., Dasari, H. P., Langodan, S., Challa, V. S., & Hoteit, I. (2016). Climatic features of the Red Sea from a regional assimilative model. *International Journal of Climatology*.

Yahel, G., Marie, D., Beninger, P. G., Eckstein, S., & Genin, A. (2009). In situ evidence for pre-capture qualitative selection in the tropical bivalve Lithophaga simplex. *Aquatic Biology*, *6*(1-3), 235-246.

Yao, F., Hoteit, I., Pratt, L. J., Bower, A. S., Zhai, P., Köhl, A., & Gopalakrishnan, G. (2014). Seasonal overturning circulation in the Red Sea: 1. Model validation and summer circulation. *Journal of Geophysical Research: Oceans*, *119*(4), 2238-2262.

Zhan, P., Subramanian, A. C., Yao, F., & Hoteit, I. (2014). Eddies in the Red Sea: A statistical and dynamical study. *Journal of Geophysical Research: Oceans*, *119*(6), 3909-3925.